micro

MDPI

Article

The Role of Bacteria in Pink Stone Discoloration: Insights from Batalha Monastery

Inês Silva [1], Cátia Salvador [1], Ana Z. Miller [1,2], António Candeias [1,3,4] and Ana Teresa Caldeira [1,3,4,*]

[1] HERCULES Laboratory & IN2PAST—Associate Laboratory for Research and Innovation in Heritage, Arts, Sustainability and Territory, University of Évora, Largo Marquês de Marialva 8, 7000-809 Évora, Portugal
[2] Instituto de Recursos Naturales y Agrobiología de Sevilla, Consejo Superior de Investigaciones Científicas, Avenida Reina Mercedes 10, 41012 Sevilla, Spain
[3] Chemistry and Biochemistry Department, School of Sciences and Technology, University of Évora, Rua Romão Ramalho 59, 7000-671 Évora, Portugal
[4] City U Macau Chair in Sustainable Heritage & Sino-Portugal Joint Laboratory of Cultural Heritage Conservation Science, University of Évora, Largo Marquês de Marialva 8, 7000-809 Évora, Portugal
* Correspondence: atc@uevora.pt

Abstract: The colonization of historical buildings and monuments by fungi, algae, and bacteria is a common phenomenon. This often leads to deterioration processes that cause either visual or structural harm. The Batalha Monastery in Portugal, a UNESCO World Heritage Site, currently shows significant surface changes to the stone architectural elements within both the Founder's Chapel and the church, including a widespread pink discoloration on the walls and columns. The main goal of this study was to analyze the biological colonization and assess the influence of bacterial communities on the biodeterioration of Ançã limestone, providing valuable insights to help conservators and restorers select the best preservation strategies for the monastery. The prokaryote population was characterized using both high-throughput DNA sequencing and culture-dependent methods and several orange-pink pigment-producing bacteria were identified, for example, *Bacillus*, *Gordonia*, *Serratia* and *Methylobacterium*, as well as *Halalkalicoccus*, an abundant archaeal genus. The pink discoloration observed could be due to biofilms created by bacteria that produce pigments, namely carotenoids. Biocolonization tests were performed using stone mock-ups, which were prepared and inoculated with the bacteria isolated in this study. These tests were designed to replicate the natural conditions of the monastery and monitor the colonization process to understand the discoloration phenomenon.

Keywords: Batalha Monastery; biodeterioration phenomena; pink discoloration; metagenomic approach; stone materials

Citation: Silva, I.; Salvador, C.; Miller, A.Z.; Candeias, A.; Caldeira, A.T. The Role of Bacteria in Pink Stone Discoloration: Insights from Batalha Monastery. *Micro* **2024**, *4*, 778–797. https://doi.org/10.3390/micro4040048

Academic Editor: Nurettin Sahiner

Received: 30 September 2024
Revised: 6 November 2024
Accepted: 12 December 2024
Published: 14 December 2024

1. Introduction

The Batalha Monastery is classified as a UNESCO World Heritage Site and is located in central Portugal [1]. Known in the country as the 'Monastery of Santa Maria da Vitória', it was built by D. João I, master of the Military Order of Aviz, in gratitude to the Virgin Mary for the victory in the Battle of Aljubarrota. It is considered an architectural masterpiece, demonstrating a perfect blend of Gothic and Manueline styles. Initial construction began in 1386 and took two centuries to complete. The building achieved the status of a royal pantheon when it received the funerary monuments of D. João I, his wife D. Filipa de Lencastre, as well as their children and grandchildren, up to D. Manuel I, in the Founder's Chapel [2]. In 1840, after the near abandonment of the monastery due to the extinction of the religious orders in 1834, the first restoration program began, and more than a century has passed since the last large-scale restoration was completed [3,4].

The microbial colonization of built heritage and monuments by fungi, algae, and bacteria is a well-known phenomenon. Cultural objects, even though they are made of

highly resistant materials, are influenced by environmental and microbiological parameters, which can modify their structure and composition. Biodeterioration caused by microorganisms results not only in the irreversible and irreparable loss of materials' physical strength, aesthetic appearance, value, and information but also, occasionally, in the destruction of the structural integrity of the valuable heritage asset. As the world's cultural heritage is unique and irreplaceable, many objects can lose part of their cultural and monetary value, making it crucial to study biodeteriorative phenomena and find appropriate mitigation strategies for the conservation and restoration of the damage caused [5–10].

The Batalha Monastery (Portugal) currently exhibits a high degree of surface alterations of the stone architectural elements both inside the church (Figure 1a,b) and the Founder's Chapel (Figure 1b), including an extensive pink coloration in the walls and columns, which appears to be the result of the formation of bacterial biofilms on the surface of the stone materials.

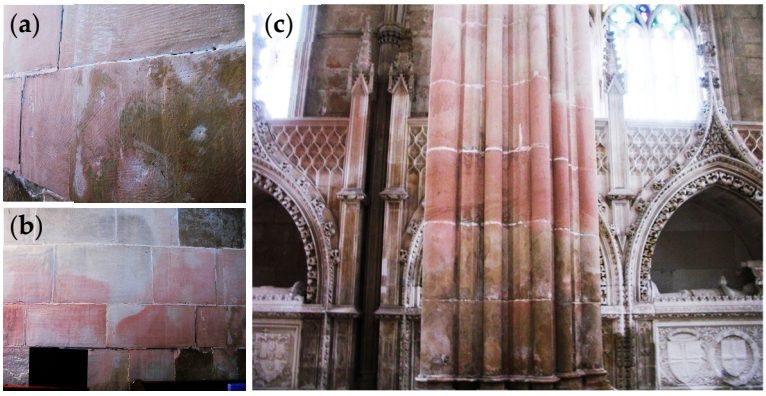

Figure 1. Surface alterations of the stone architectural elements both inside (**a**,**b**) the church and (**c**) the Founder's Chapel at Batalha Monastery.

Since some microbes might generate colored substances, they can cause chromatic changes and permanent staining. Carotenoids, which are highly unsaturated isoprene derivatives of tetraterpenoids and are mostly produced by bacteria but are also produced by filamentous fungi [11], yeasts [12], algae [13], and lichens [14], are an example of these colored molecules. Carotenoids exhibit yellow, orange, and red colors and are the most abundant class of dyes found in nature. This type of pigment plays a key role in the extraction of light energy, quenching photosensitizers to protect organisms from oxidative damage, interacting with singlet oxygen and scavenging peroxy radicals to prevent the formation of dangerous oxygen species, and stabilizing specific pigment–protein complexes [15–18].

Thus, to identify the phenomena that promote the appearance of these stains on the walls, a multidisciplinary approach was adopted, incorporating both culture-dependent and -independent methods, as well as spectroscopy and colorimetry techniques. The main objectives of our research were to (i) characterize the bacteria colonizing the stone surfaces, (ii) evaluate the distribution patterns of the bacteria across different sampling zones, (iii) characterize the pigments produced by these microorganisms, (iv) replicate the discoloration process observed in the monument, and (v) identify potential solutions to the staining problem.

2. Materials and Methods

2.1. Sampling Process

The Monastery of Batalha is a Dominican monastery, constituting a cultural, tourist, and devotional architectural complex, located in the Portuguese village of Batalha, in the district of Leiria, in the central region of Portugal (39°39′ 32″ N 8°49′33″ W).

The sampling process focused on two representative areas of the monastery, selected due to their evident signs of contamination and alteration, corresponding to (1) walls and columns of the Church (samples A1 and B1) and (2) walls and columns of the Founder's Chapel (samples A2, A3, B2, B3, B4, B5, and B6). The samples were collected under the coordination of conservators and restorers, fulfilling the conservation requirements and minimizing the structural and aesthetic impact on the monument, collecting the minimum quantity necessary for testing. Non-invasive methods (swab samples identified with letter B) and semi-invasive methods (collection of stone microfragments, taken with sterilized scalpels, identified with letter A) were used to collect the samples, under semi-aseptic conditions (collection carried out with sterile material, but in an external environment). Stone microfragments were collected close to losses or cracks to avoid additional damage.

2.2. Culture-Dependent Methods

The swabs were cultivated aseptically in Nutrient Agar (NA, HIMEDIA—5 g/L peptic digestion animals, 1.5 g/L beef extract, 1.5 g/L yeast extract, 5 g/L sodium chloride, and agar 15 g/L). The plates were sealed with biofilm and incubated at 30 °C for 24 to 48 h for bacterial growth. To detect slow bacteria growth, the inoculated Petri dishes remained in incubation for longer, up to 30 days, and were monitored periodically. Pure bacterial strains were obtained after successive subcultures of colonies that grew during that period with different macromorphological characteristics.

The identification of microbiological isolates was based on macroscopic characteristics, such as texture, colony color, cell dimensions, and morphology. The bacterial strains isolated from the stone samples were cataloged and stored in the culture collection HERCULES-Biotech laboratory, University of Évora, and were maintained at 4 °C.

Prokaryotic DNA was extracted following the protocol outlined by Rinta-Kanto et al. (2005) [19]. The PCR products were then purified and sequenced by the external service provider STAB VIDA (Lisbon, Portugal). The nucleotide sequences were aligned with those retrieved from the GenBank (NCBI) databases, and homology analysis was performed using the BLASTN 2.8.0 program.

2.3. Culture-Independent Methods

The NGS approach required the extraction of metagenomic DNA from the original microsamples, which was performed using the Soil DNA Purification Kit (OMNI Inc., Kennesaw, GA, USA), according to the manufacturer's instructions. The DNA was quantified by a fluorometric technique with the Quantus™ Fluorometer equipment (E6150, Promega, Madison, WI, USA) using the QuantiFluor® dsDNA System Kit (E487, Promega, Madison, WI, USA).

Bacterial communities were analyzed through Illumina sequencing targeting the V3-V4 region of the 16S rRNA gene. The DNA was initially amplified for the hypervariable regions using specific primers and subsequently underwent limited-cycle PCR t o incorporate sequencing adaptors and dual indexes. For bacteria, the following primers were used: forward primer Bakt_341F (5′-CCTACGGGNGGCWGCAG-3′) and reverse primer Bakt_805R (5′-GACTACHVGGGTATCTAATCC-3′) [20,21].

The procedures for DNA amplification, purification, quantification of amplicons, and data analysis were performed according to Silva et al. (2024) [22].

2.4. Bacterial Biofilm Formation Capacity Assay

The ability to form bacterial biofilms was determined using the crystal violet method, which is a classic method for testing this ability from bacterial isolates. The halophilic isolates were incubated at 30 °C, 100 rpm for 7 days in HS liquid medium (250 g NaCl, 20 g $MgSO_4 \cdot 7H_2O$, 3 g trisodium citrate $\cdot 2H_2O$, 2 g KCl, and 10 g bacteriological peptone, pH 6.5–7.4).

After the growth of the liquid cultures, 90 µL of HS medium and 10 µL of the bacterial isolates were added to a 96-well polystyrene plate, which was left to incubate at 37 °C for

72 h. After this period of time, the medium was discharged from the plate where the culture was incubated. The wells were stained with 125 µL of crystal violet (0.1%) for 15 min. Excess dye was discharged, 200 µL of acetic acid (30% v/v) was added for solubilization, and the absorbance was read at 595 nm.

To evaluate differences in the capacity of formation of biofilms by the different bacteria isolates, a one-way variance analysis (ANOVA) was performed with the software IBM SPSS® Statistics (version 25.0) for Windows (Microsoft Corporation, Redmond, WA, USA). The homogeneity of population variances was confirmed by Levene's test, and multiple comparisons of means were measured using Tukey's test. A *p*-value less than 0.05 was considered statistically significant.

2.5. In Situ Biocolonization Tests

2.5.1. Inoculation

Biocolonization tests were performed by preparing stone mock-ups that were inoculated with the bacteria isolated during the study. This aimed to simulate the monastery's natural conditions and monitor the colonization process, providing insights into the discoloration phenomenon.

The limestone mock-ups (6 cm^2) were washed, dried, and sterilized. To make a liquid culture, the bacterial isolate (CCLBMBatB3) was diluted in 50 mL of HS liquid medium and was incubated at 30 °C, 100 rpm, for 7 days. The test was carried out using two different mock-ups, inoculated with the same bacterial isolate: one of them kept under sunlight, on an incubator shaker, the other kept in darkness, inside an incubator. Both pieces of equipment were kept at 30 °C.

Then, 1×10^{10} CFU/mL of these bacterial suspensions was applied to the stone, spreading it evenly over the entire stone surface. The assay was monitored by inoculating 1 mL of HS culture medium every two days, and the growth of biofilms on the stone was monitored every day. A control stone was included in the tests, without any bacterial inoculation.

2.5.2. Colorimetry Approach

The color change of each mock-up used in the simulation tests was measured by a non-invasive spectrophotometer, KONICA MINOLTA CM-700d (Japan, Osaka). For the reference measurements, the colorimeter was previously calibrated in terms of black and white, and the results were checked to ensure that the L*a*b* values for the black and white referenced samples were approximately (100, 0, 0) and (0, 0, 0), respectively.

The results obtained in the CIE L*a*b* color space defined by the CIE represent the average of five measurements carried out on the stone surface. The chromatic coordinates measured were L*, which represents luminosity (0–100); a*, which represents the red/green axes; and b*, which represents the yellow/blue hue axes (0–100). The C* coordinate, derived from the previous color space (CIE L*C*h*), which represents chroma (color purity or saturation), was also analyzed [23]. Changes in these parameters were determined by calculating the E parameter (total color difference), using the following equation:

$$\Delta E = ((\Delta L)^2 + (\Delta a)^2 + (\Delta b)^2)^{1/2}\, \Delta L = (L_2 - L_1);\ \Delta a = (a_2 - a_1);\ \Delta b = (b_2 - b_1)$$

2.5.3. Raman Spectroscopy

To complement the tests, selected samples were analyzed by Raman spectroscopy to confirm the identification of the pigments in vitro and in situ, using a Horiba Xplora Raman spectrometer coupled to an Olympus microscope. Raman spectra were acquired in extended mode in the 0–2500 cm^{-1} range. A laser with a wavelength of 785 nm and a 10% filter was applied. Raman spectra were obtained by accumulating 10 acquisitions of 30 s with a spectral resolution of 5 cm^{-1}. No sample preparation was required. The spectra were analyzed with the equipment software (LabSPEC 5 from Horiba Jobin Yvon, France, Longjumeau).

2.6. In Situ Pigment Cleaning Tests

In an attempt to eliminate the carotenes produced by bacteria on the stone, cleaning tests were carried out on the limestone mock-ups.

A cleaning solution was prepared with a mixture of pure isopropyl alcohol (E.Merck) and distilled water, in different concentrations (50, 25, 10, and 5%), and applied to the stones (500 µL/2 cm^2) where the pigmented bacterial biofilm was observed, to evaluate the pigment removal capacity. The effectiveness of the cleaning solution was measured using colorimetry, as described in point 2.5.2 of the methodology.

3. Results and Discussion

3.1. Characterization of Microbiota Through Culture-Dependent Methods

Culture-dependent methods allowed the characterization of the cultivable isolated population (Table 1), composed of prokaryotic microorganisms, producing interesting pigments.

Table 1. Macromorphological characteristics of bacterial isolates with identification by Sanger sequencing.

Sample	Macroscopic Characteristics		Bacterial Strain	Most Probable Identification	GenBank Accession Number
	Front	Back			
B1		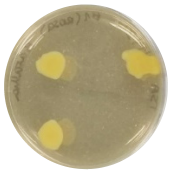	CCLBMBat1	*Pseudomonas* sp.	PQ095922
	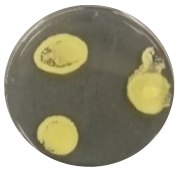	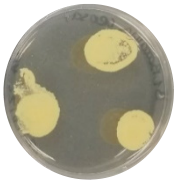	CCLBMBatB1-2	*Kocuria* sp.	PQ144780
B2		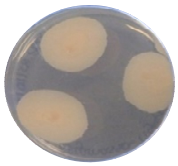	CCLBMBatB2	*Bacillus* sp.	PQ144790
	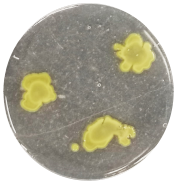	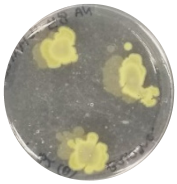	CCLBMBatB2-2	*Citricoccus* sp.	PQ144849
B3		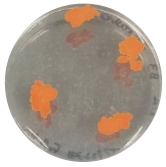	CCLBMBatB3	*Gordonia* sp.	PQ144851

Table 1. *Cont.*

Sample	Macroscopic Characteristics		Bacterial Strain	Most Probable Identification	GenBank Accession Number
	Front	Back			
B4	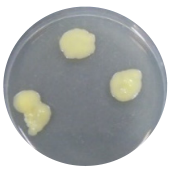	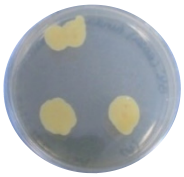	CCLBMBatB4-1_2	*Micrococcus* sp.	PQ144861
	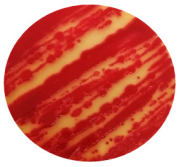		-	*Serratia* sp.	SAMN42837401

Although conventional culture methods are not sufficient for the complete characterization of the microbiota, one of the main advantages of culture isolation is that different organisms can be preserved for further testing, to understand their ecological functions and identify specific interactions with materials and other organisms. Moreover, isolation is essential for obtaining new strains for further characterization and description, thereby enhancing our current understanding of true microbial diversity.

The results of this analysis are described below.

Using culture-dependent methods, it was possible to identify the cultivable population present on the degraded areas of stone samples. The isolated strains were identified as *Pseudomonas* sp. (CCLBMBat1), *Kocuria* sp. (CCLBMBatB1-2), *Bacillus* sp. (CCLBMBatB2), *Citricoccus* sp. (CCLBMBatB2-2), *Gordonia* sp. (CCLBMBatB3), *Micrococcus* sp. (CCLBMBatB4-1_2), and *Serratia* sp. (PRJNA1140600).

Sample B2 showed a high percentage of identity with *Bacillus* sp., which is a Gram-positive, aerobic, neutrophilic, saprophytic, spore-forming bacterium found in diverse habitats but commonly considered as a soil bacterium [24]. *B. megaterium* spores, for example, contain a unique reddish pigment (identified as being consistent with a carotenoid structure) in their membranes that is not found in other species. This pigment may play a role in the stability of the spore membranes of this microorganism and therefore may be important in the resistance properties of the spores [25–27].

Gordonia sp., identified in sample B3, is a Gram-positive, aerobic, and desulfurizing actinomycete [28], orange-pink in color and capable of using alkanes as a carbon source. It is described as producing strong pigmentation, associated with reddish carotenoids, especially when exposed to intense light [29,30]. Of the different carotenoids produced, three were identified as canthaxanthin (reddish pigment), astaxanthin (salmon pink carotenoid pigment), and lutein (yellow-orange pigment) [16].

The genus *Serratia* belongs to the Enterobacteriaceae [31] family and produces pink/red pigmentation known as prodigiosin [32].

3.2. Characterization of Microbiota Through Culture-Independent Methods

Due to the known limitations of culture-dependent methods for the purpose of this study, a phylogenetic metagenomic approach was used through Next-Generation Sequencing (NGS), which has evolved exponentially in recent years, allowing the characterization of microbial diversity, but also a better understanding of the functions, activities, and dynamics of microbial communities. This method makes use of small subunit ribosomal DNA genes, such as 16S, which are found in all prokaryotes and offer a reliable way to identify microorganisms [33].

Considering the set of all samples, the dominant phylum (Figure 2a) is Firmicutes (69.40%), followed by Euryarchaeota (22.14%), Proteobacteria (5.14%), Actinobacteria (2.52%), and 0.80% for "others" (generic designation corresponding to species with lower representation).

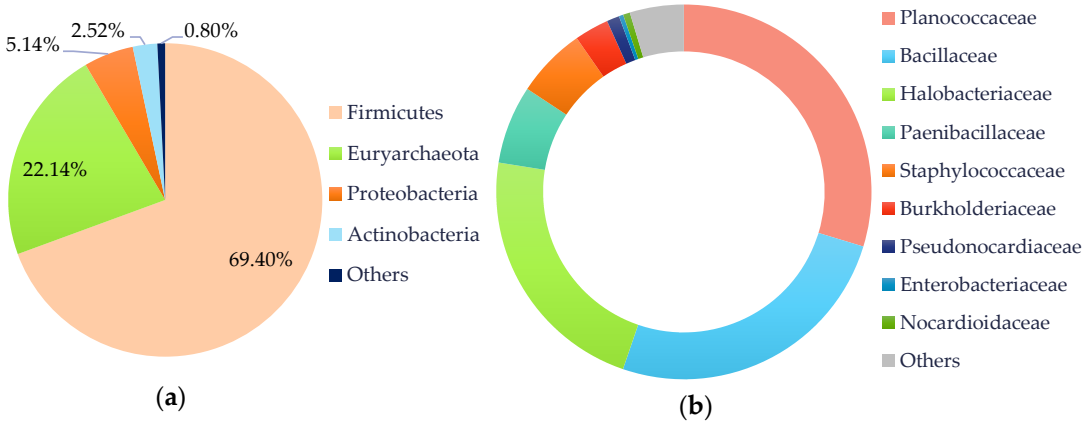

Figure 2. Predominant prokaryote (**a**) phyla and (**b**) families on the pink biofilms.

The results show that the prokaryotic population present on the Batalha Monastery belongs to the following families (Figure 2b): Planococcaceae (29.72%), Bacillaceae (25.55%), Halobacteriaceae (22.25%), Paenibacillaceae (6.76%), Staphylococcaceae (6.05%), Burkholderiaceae (2.97%), Pseudonocardiaceae (1.09%), Nocardioidaceae (0.60%), and Enterobacteriaceae (0.37%). Families classified as "others" represented 4.65% of the population.

At the genus level (Figure 3), the most frequently identified genus was *Bacillus* (25.06%), followed by *Halalkalicoccus* (21.91%), *Sporosarcina* (12.63%), *Rummeliibacillus* (7.98%), *Paenibacillus* (6.82%), *Planococcaceae_incertae_sedis* (6.23%), *Staphylococcus* (6.07%), *Ralstonia* (2.17%), *Paenisporosarcina* (1.32%), *Lysinibacillus* (0.95%), *Oceanobacillus* (0.86%), *Burkholderia* (0.80%), *Haloechinothrix* (0.77%), *Domibacillus* (0.69%), *Kribbella* (0.58%), *Halorientalis* (0.27%), *Halococcus* (0.26%), *Methylobacterium* (0.24%), *Tissierella* (0.12%), and *Paucisalibacillus* (0.01%). A total of 4.27% were classified as "others".

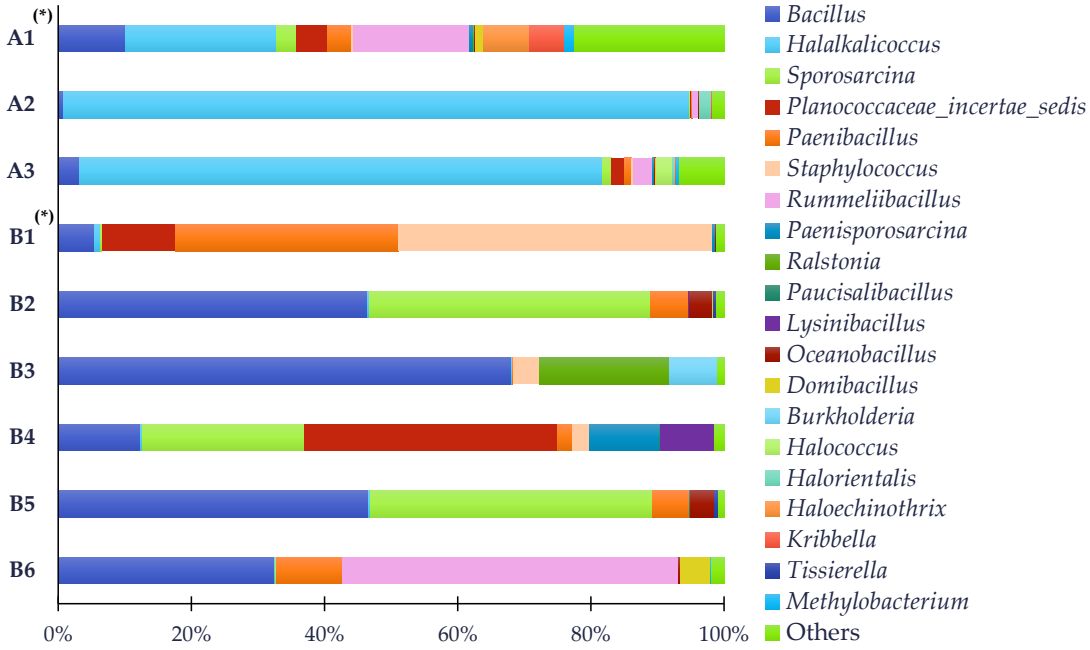

Figure 3. Predominant prokaryote genera on the pink biofilms; the symbol (*) represents the samples collected in the monastery church.

Bacillus was identified in all of the samples of this study, remarkably in samples B2 (46.48%), B3 (68.14%), B5 (46.65%), and B6 (32.52%). This genus consists of aerobic, spore-forming, rod-shaped bacteria with great metabolic versatility [34], thriving in almost all natural environments (soil, water, rocks, etc.). *Bacillus* endospores are highly resistant to a variety of environmental stress factors [27,35], and the prevalence of this genus is closely linked to its ability to form spores, providing significant advantages for microbial survival and growth in harsh environments. It has been frequently documented in a wide range of cultural heritage objects, including wall paintings, frescoes, catacombs, paintings, and stone monuments [36]. Kiel and Gaylarde (2006) reported that some strains of *Bacillus* produce acids and surfactants with self-emulsifying activity, indicating that they have the ability to accelerate processes that lead to the degradation of stone substrates [37].

In the genus *Bacillus*, there is a wide spectrum of species that produce carotenoid pigments (such as *B. firmus*, *B. megaterium*, *B. licheniformis*, *B. aquimaris*, *B. atrophaeus*, *B. indicus*, among others) with a predominance of yellow, orange, and pink, with the intensity of the color varying depending on the species and the corresponding strain. This type of pigment in *Bacillus* has a protective effect against UV radiation, as antioxidants, and located in membranes, carotenoids are capable of eliminating reactive oxygen species generated by radiation [26,27].

The genus *Halalkalicoccus* was identified mainly in samples A1 (22.71%), A2 (93.97%), and A3 (78,60%). Most species in this genus are pigmented pink, orange, or red due to carotenoid pigments, and they have been well documented in numerous historical monuments, especially in cases of contamination involving pink discoloration and the production of saline efflorescences [38–44]. Salts, along with other factors such as temperature, humidity, and sunlight exposure, play a crucial role in influencing microbial communities on various substrates. Specifically, high salt concentrations create osmotic stress conditions that favor halotolerant and halophilic microorganisms. This high salinity alters community structure by selecting for species with specialized adaptations, which can significantly impact biofilm development and microbial interactions [22]. As a result, high-salinity environments often lead to the predominance of halophilic taxa, such as *Halalkalicoccus*, which are well adapted to thrive under these conditions.

In addition to the genus, some bacterial species were identified by sequencing the V3-V4 region of the 16S rRNA gene, which are relevant for the production of carotenoids and pink pigments and, in this context, can contribute to the formation of biofilms, leading to the pink discoloration observed on the monument. Some of the relevant bacteria were *Halalkalicoccus tibetensis*, *Rummeliibacillus stabekisii*, *Bacillus firmus*, *Bacillus aryabhattai*, and *Bacillus cereus*.

Bacillus firmus has been scientifically correlated with cultural heritage, as it produces pink pigments, including carotenoids like astaxanthin [26,45–47]. Another species, *Bacillus aryabhattai*, is a UV-resistant and halotolerant rhizobacterium with a strong capacity for biofilm formation under high-salinity conditions [48,49].

Bacillus cereus produces a reddish-pink pigment (pulcherrimin a) and has been documented throughout the world mainly (i) in deteriorated wall paintings [50,51]; (ii) on biodeteriorated stone surfaces, producing a biofilm that leads to the phenomenon called biopitting [52,53]; (iii) as a biodeteriogen in textiles, especially wool fibers [54]; (v) as a significantly abundant microorganism that causes serious biodeterioration in limestone—as it has the capacity to dissolve calcium carbonate [55].

Halalkalicoccus tibetensis is a haloalkaliphilic archaea that thrives in environments with high pH and salinity, and it produces orange pigments [56].

The HTS approach has proven to be a valuable complement to traditional microbiological methods by providing detailed and high-quality data. However, while the strains isolated through cultivation do not exactly align with the top 20 genera identified in the NGS data, it remains crucial to continue characterizing the cultivable population for conducting laboratory simulation assays.

3.3. Determination of Bacterial Biofilm Formation Capacity

The ability of the bacterial isolates to form biofilms was assessed using the crystal violet staining method, a widely employed technique for biofilm quantification. This method involves staining biofilms in microplate wells (Figure 4) to evaluate the early stages of biofilm formation. The intensity of the resulting stain is directly proportional to the biofilm biomass, providing a reliable measure of biofilm production [57–59].

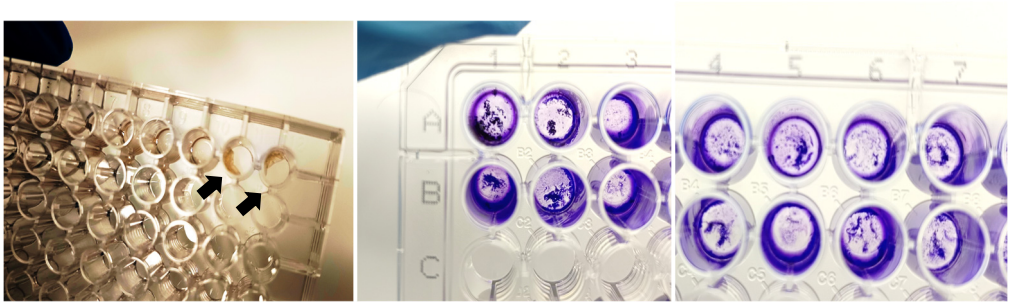

Figure 4. Formation of biofilms on microplates by the bacterial isolate Gordonia.

The ability of the bacterial isolates to form biofilms was determined spectrophotometrically, by reading the absorbance at 595 nm. The results are presented in Figure 5.

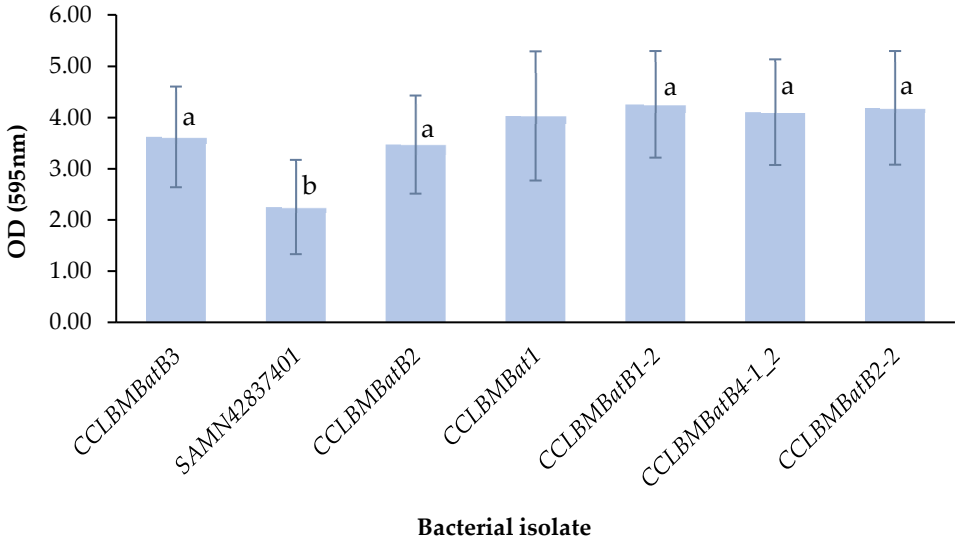

Figure 5. Determination of biofilm formation capacity. The values shown are the mean ± standard deviation of 16 replicates. Different letters (a or b) indicate different levels of significance.

To compare the biofilm formation capacities of the different bacterial isolates, a one-way ANOVA followed by Tukey's post hoc test was conducted at a significance level of 0.05. This analysis revealed statistically significant differences between the samples ($p < 0.05$). Specifically, the isolate SAMN42837401 exhibited a significantly lower absorbance value, as shown in Figure 5, indicating a reduced capacity for biofilm formation compared to the other isolates. In contrast, the remaining isolates—CCLBMBat1, CCLBMBatB2, CCLBMBatB1-2, CCLBMBatB4-1_2, CCLBMBatB2-2, and CCLBMBatB3—demonstrated similar biofilm-forming abilities.

Given the extended duration of the biocolonization tests and the pigment production by the other bacteria, which primarily produced yellow and cream-colored pigments, the isolate CCLBMBatB3, a member of the genus *Gordonia* and producer of pink-orange carotenoids, was selected for subsequent in situ testing.

3.4. Assessment of Carotene Production in In-Situ Biocolonization Tests

The result of the production of the pigmented bacterial biofilm is illustrated below, in Figure 6a,b.

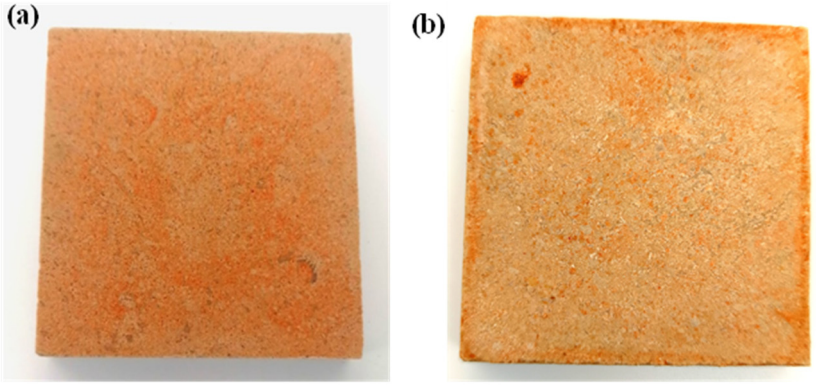

Figure 6. Production of pigments in the stone mock-up by isolate CCLBMBatB3 (**a**) kept in the dark and (**b**) exposed to sunlight.

3.4.1. Measurement of the Colorimetric Parameters

To evaluate the difference in color between the two stones where the colored biofilm was produced and the control stone, in situ analyses were carried out using colorimetric techniques.

The measurement of colorimetric parameters in the stone kept in the dark and in sunlight, using the CIELAB system and the determination of ΔE, is shown in Table 2. These parameters are also represented in the CIELAB color space (Figure 7).

Table 2. Measurement of colorimetric parameters, using the CIELAB system and determination of ΔE.

Stone Sample	L*	a*	b*	ΔE [1]
Control	82.48 ± 0.68	2.19 ± 0.06	10.24 ± 0.13	-
Stone (dark conditions)	67.39 ± 0.25	14.46 ± 0.76	24.21 ± 0.66	23.95 ± 0.85
Stone (bright conditions)	70.33 ± 2.40	20.68 ± 4.38	28.57 ± 4.64	28.74 ± 6.61

[1] Based on the difference between stained stones and control stone.

The CIELAB color space (Figure 7) uses three values to determine each color (L*a*b*) and is based on the vision-opposing color theory, which states that a color cannot be green and red at the same time, nor blue and yellow at the same time [60].

The results clearly suggest a change in the original color of the stone, both in terms of visualization with the naked eye and observation of the Cartesian coordinates and also in the measurement of ΔE, calculated from the comparison between the CIELAB parameters of the two stones. The high ΔE values (>16 units) indicate that the original color of the stone surfaces in stained regions is significantly compromised. The areas with the development of biofilms were those that showed significant changes in color, which is largely responsible for the aesthetic damage observed.

There is also a slight difference in the colorimetric parameters and the color observed between the stone exposed to sunlight and the stone kept in the dark during the test. The first presents a higher ΔE (28.74) than the second (23.95), and a more vivid color was also observed in the stone exposed to light.

The slightly more intense color in the stone exposed to sunlight can possibly be justified by previous studies, which suggested that *Gordonia* sp. is a light-induced producer of carotenoids, based on the selective production of reddish color that is more intense under higher light and whose growth increases under these conditions [61]. Fernandes et al.

(2018) also highlighted the importance of incubation time for the development of pigments, demonstrating that longer cultures, exposed to light, achieve a higher concentration of carotenoids [62].

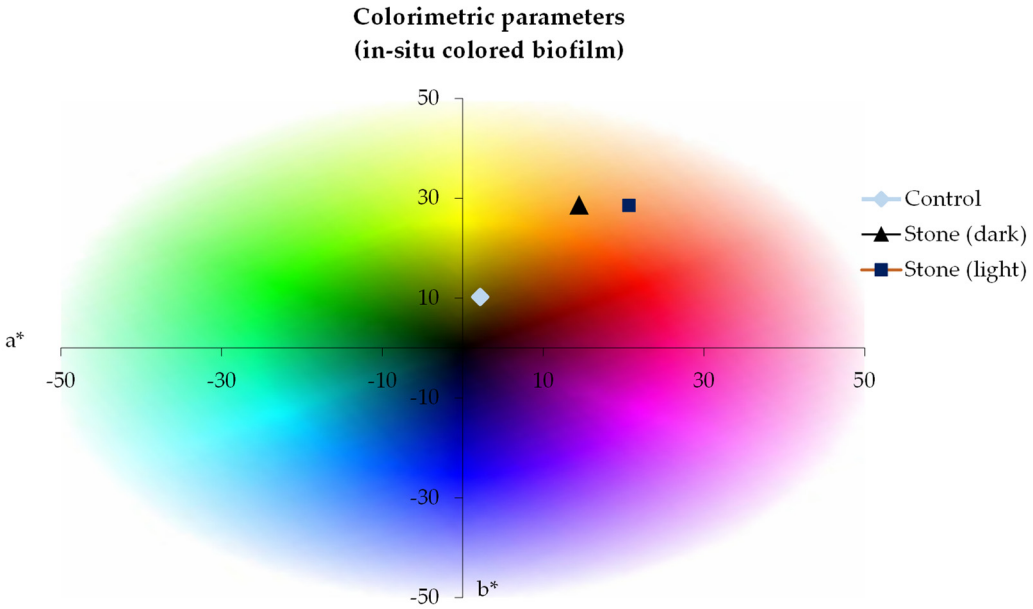

Figure 7. CIELAB color spectrum and color representation of colored stones and control.

3.4.2. RAMAN Spectroscopy

Raman spectroscopy analyses were carried out to support previous results. This approach enables the detection of carotenoids, which are compounds generated by the metabolic activity of particular microorganisms. As previously stated, carotenoids may range in color from yellow to red; therefore, the presence of these molecules is likely responsible for the reddish stains in the stone.

Raman spectroscopy was applied (i) in vitro, to confirm the production of carotenes by the isolate CCLBMBatB3, *Gordonia* sp., and (ii) in situ, in order to characterize the pigments that were produced in the biofilm developed on the stones.

The results obtained by this technique are illustrated and described below, in Figures 8–10 for in vitro and in situ analysis, respectively.

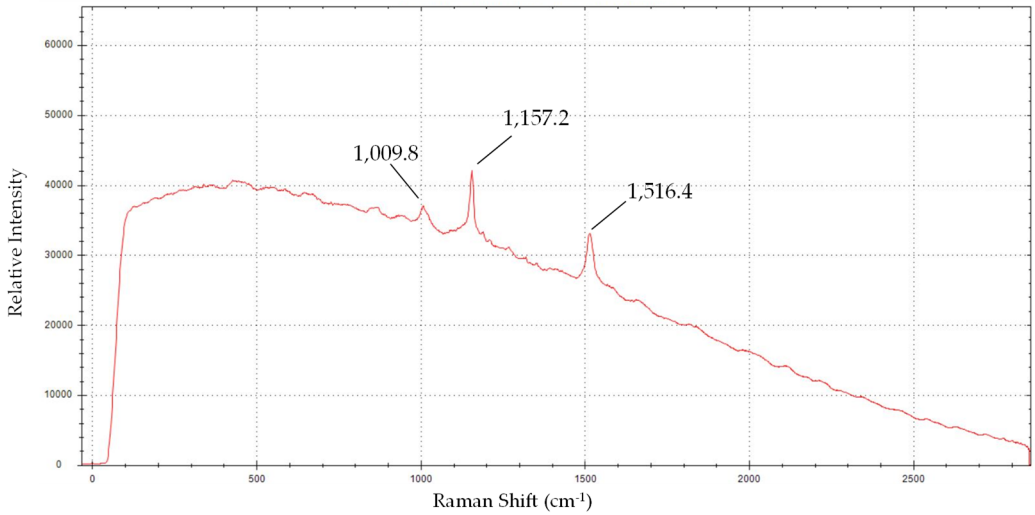

Figure 8. Raman spectrum of in vitro bacterial isolate CCLBMBatB3.

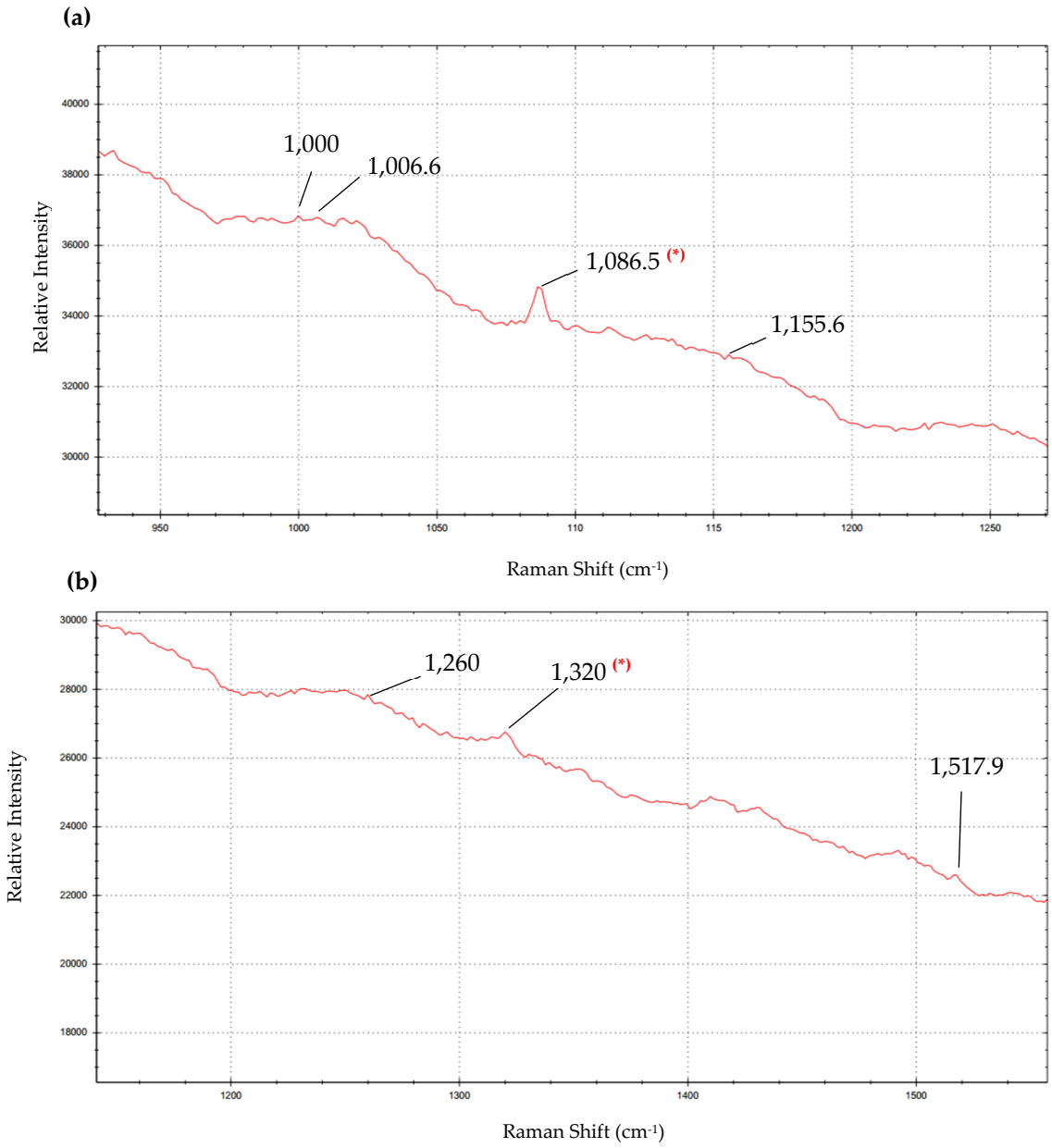

Figure 9. In situ Raman spectra of the stone kept in the dark considering the scales (**a**) 930–1270 cm^{-1} and (**b**) 1160–1560 cm^{-1}. The connotation (*) represents peaks corresponding to calcite.

According to the literature, for natural carotenoids, regardless of the end group, the Raman spectrum is dominated by three characteristic bands at ~1520, ~1160, and ~1000 cm^{-1} [63].

The Raman spectrum of the CCLBMBatB3 (*Gordonia* sp.) isolate in vitro (Figure 8) allowed the identification of the bands 1009.8, 1157.2, and 1516.4 cm^{-1}, characteristic of carotene compounds [64,65], so spectrophotometric analysis revealed that these microorganisms have the ability to promote pigmentary changes in culture.

In the limestone mockup kept in the dark (Figure 9), the peaks 1000, 1006.6, 1155.6, 1260, and 1517.9 cm^{-1} were identified, equally characteristic of carotene compounds. In the stone exposed to sunlight (Figure 10), the peaks 1000, 1160.6, 1260, and 1279.7 cm^{-1} were identified, corresponding to the identifying peaks of carotenes.

Gordonia sp., the bacterial isolate used in the test, is described as producing the well-known pigments lutein, canthaxanthin (4,4′-diketo-β-carotene), and astaxanthin (3,3′-dihydroxy-β,β′-carotene-4,4′-dione) [16]. The theoretical values of these compounds were

identified as 966, 1009, 1159, 1195, 1277, 1448, and 1520 cm^{-1} for astaxanthin [66]; 1008, 1159, and 1525 cm^{-1} for lutein [67,68]; and 1512, 1269, 1189, 1159, and 999 cm^{-1} for canthaxanthin [69].

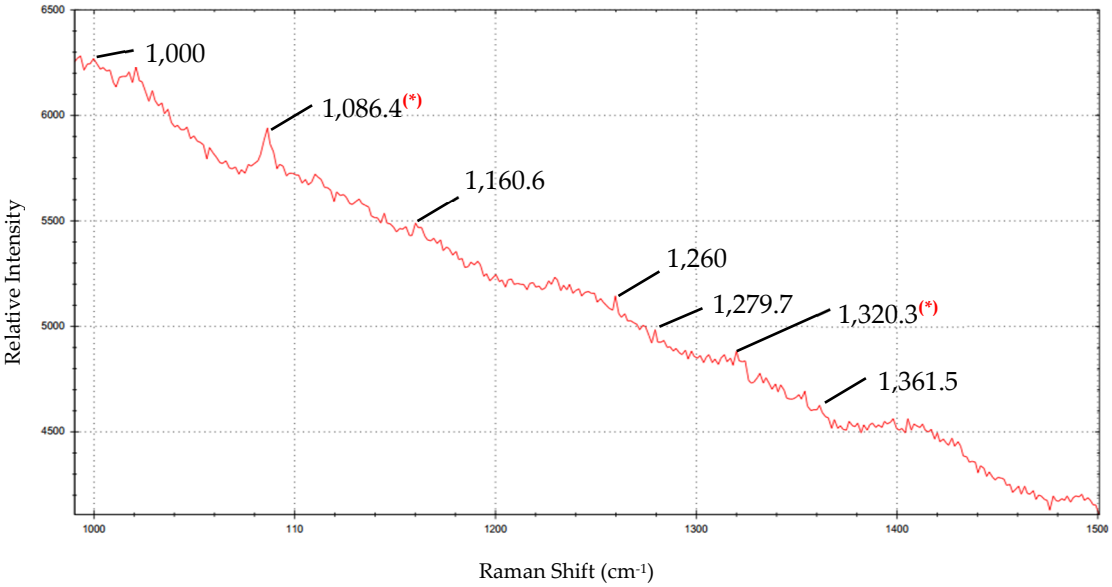

Figure 10. In situ Raman spectra of the stone exposed to the sunlight. The connotation (*) represents peaks corresponding to calcite.

In fact, the carotenes lutein, canthaxanthin, and astaxanthin present similar resonance Raman spectra in terms of Raman shifts and relative signal intensities [67].

3.5. Evaluation of Cleaning Solution Effectiveness in Pigment Removal

3.5.1. Stone Mockup Kept in the Dark

Cleaning material-based works of art involves preserving the aesthetics, legibility, and physical and chemical stability of the materials [70]. The results before and after cleaning the stone and the resulting colorimetric parameters are represented in Figure 11 and Table 3, respectively.

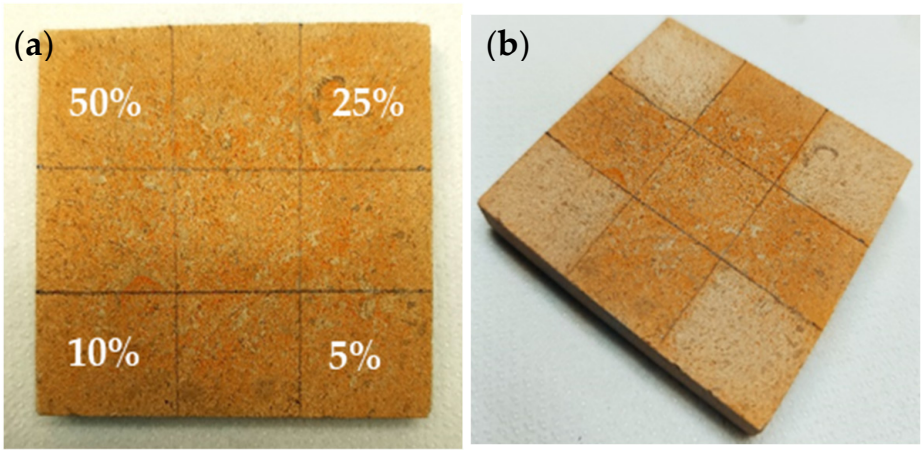

Figure 11. Cleaning test on stone (in conditions of darkness) stained by bacterial biofilms: (**a**) before and (**b**) after the cleaning process.

Table 3. Measurement of colorimetric parameters: cleaning test with the stone mockup in conditions of darkness.

Sample	L*	a*	b*	ΔE [1]
Stone (dark)	67.39 ± 0.25	14.46 ± 0.76	24.21 ± 0.66	-
Sol. 50%	77.82 ± 0.50	5.33 ± 0.18	15.51 ± 0.24	16.37 ± 0.44
Sol. 25%	74.73 ± 0.86	5.49 ± 0.24	16.40 ± 0.27	13.99 ± 0.68
Sol. 10%	71.95 ± 3.90	4.76 ± 0.45	15.40 ± 1.12	14.40 ± 0.74
Sol. 5%	74.32 ± 0.16	4.71 ± 0.07	15.83 ± 0.30	14.60 ± 0.26

[1] based on the difference between the spaces where the cleaning solution was applied and the stained stone.

Based on Figure 11 and Table 3, it can be seen that the cleaning solution efficiently removed carotenes from the stone at all concentrations used. The 50% concentration appears to produce the best results (ΔE = 16.37), although the other concentrations also have sufficiently high values to allow effective removal, which is an advantage when they are applied directly to monumental stone. Figure 12 below also illustrates, through reflectance measurement, the production of similar results between the different concentrations used in cleaning.

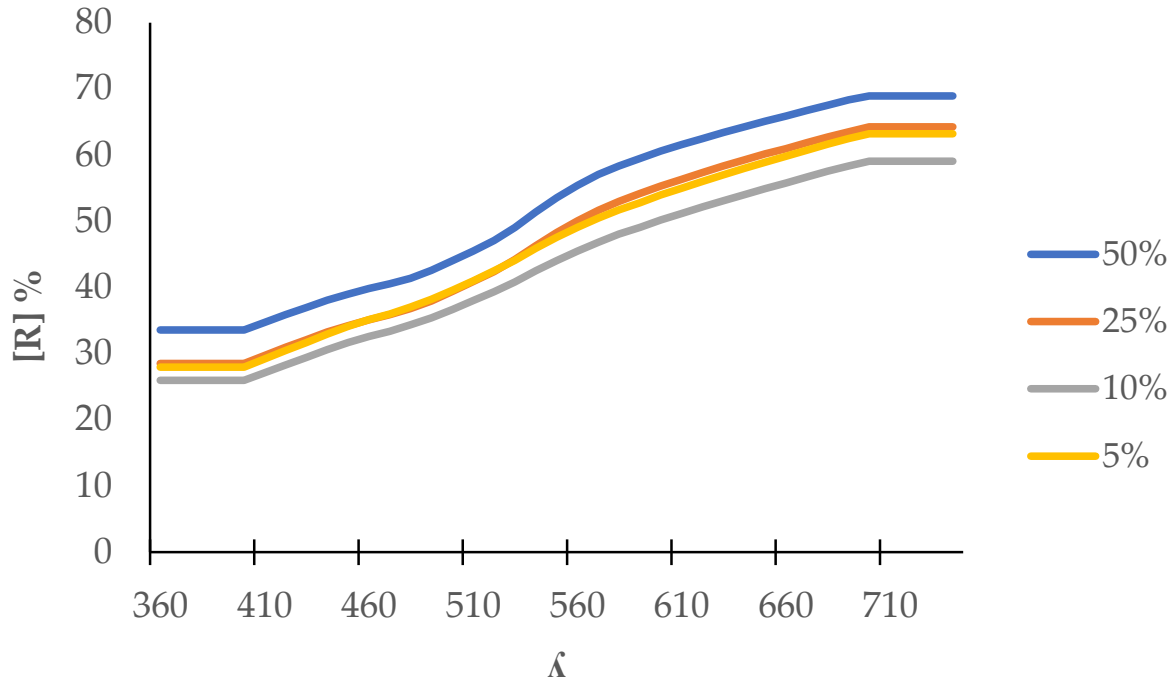

Figure 12. Measurement of reflectance (%) for the cleaning solutions (stone kept in the dark).

Sample reflectance (%R) corresponds to the output of the spectrophotometer and is, by definition, a measure of the ability of a surface to reflect light or other electromagnetic radiation. Reflectance measurement has been used to detect biofilm-related color changes and to assess the extent of microbial colonization on various substrates. Additionally, the relationship between increased reflectance and biofilm removal efficacy has been documented in previous studies, demonstrating that reflectance measurements can provide a quantitative assessment of surface cleanliness after biofilm removal [71–73].

In this case, the stone stained by the pigments will have a characteristic reflectance, which will be influenced by the presence of these pigments. Generally, microbial biofilms tend to reduce the reflectance of the surface, making it darker or more opaque. If the cleaning process is effective, it will remove the biofilms, exposing the original surface of the stone. The reflectance of the cleaned stone will generally be higher, as the original stone surface reflects more light than a surface covered by biofilms. Thus, an increase in reflectance after cleaning generally indicates that the surface of the stone was effectively cleaned, removing most of the pigments.

As shown in Figure 12, the solution with 50% isopropyl alcohol exhibited the highest colorimetric parameters for delta E and reflectance, suggesting that this concentration produced the greatest differences and was the most effective at removing carotenoid pigments. However, all cleaning solutions were effective and produced similar results, indicating they should be suitable for removing biofilm-induced coloration from stone surfaces.

3.5.2. Stone Mockup Exposed to Sunlight

The results relating to the cleaning test on the stone in bright conditions are illustrated in Figure 13 and Table 4.

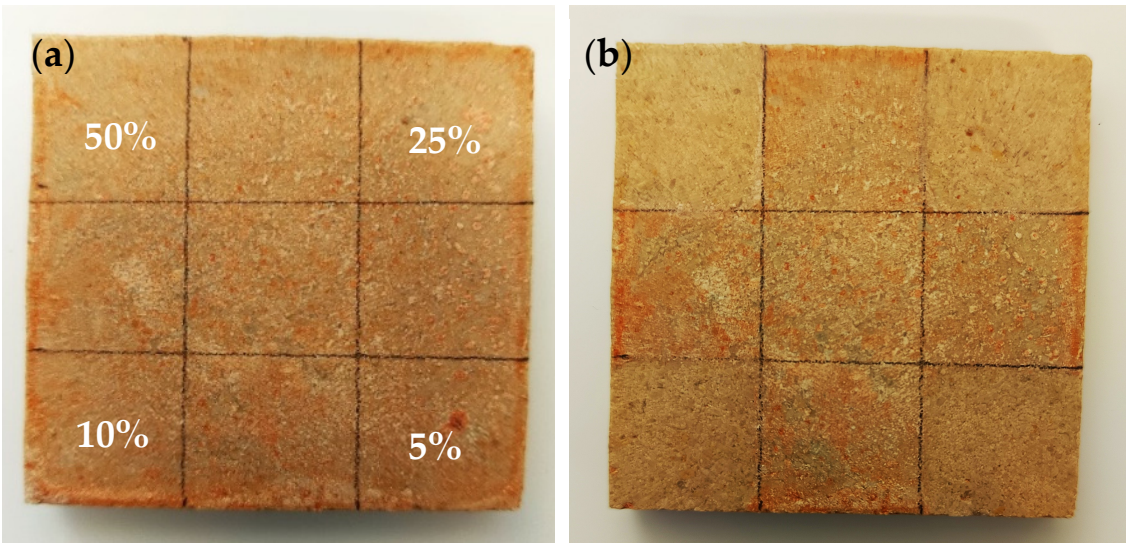

Figure 13. Cleaning test on stone (in bright conditions) stained by bacterial biofilms: (**a**) before and (**b**) after the cleaning process.

Table 4. Measurement of colorimetric parameters: cleaning test with the stone mockup in bright conditions.

Sample	L*	a*	b*	ΔE [1]
Stone (bright)	70.33 ± 2.40	20.68 ± 4.38	28.57 ± 4.64	-
Sol. 50%	76.51 ± 1.01	5.33 ± 0.38	16.65 ± 0.82	20.42 ± 0.93
Sol. 25%	75.47 ± 0.71	5.02 ± 0.15	17.05 ± 0.47	20.12 ± 0.47
Sol. 10%	75.32 ± 0.44	5.35 ± 0.23	16.84 ± 0.23	19.24 ± 0.28
Sol. 5%	75.22 ± 0.85	4.68 ± 0.32	16.55 ± 0.82	20.61 ± 0.90

[1] based on the difference between the spaces where the cleaning solution was applied and the stained stone.

Figure 14 below also illustrates, through reflectance measurement, the production of similar results between the different concentrations used in cleaning.

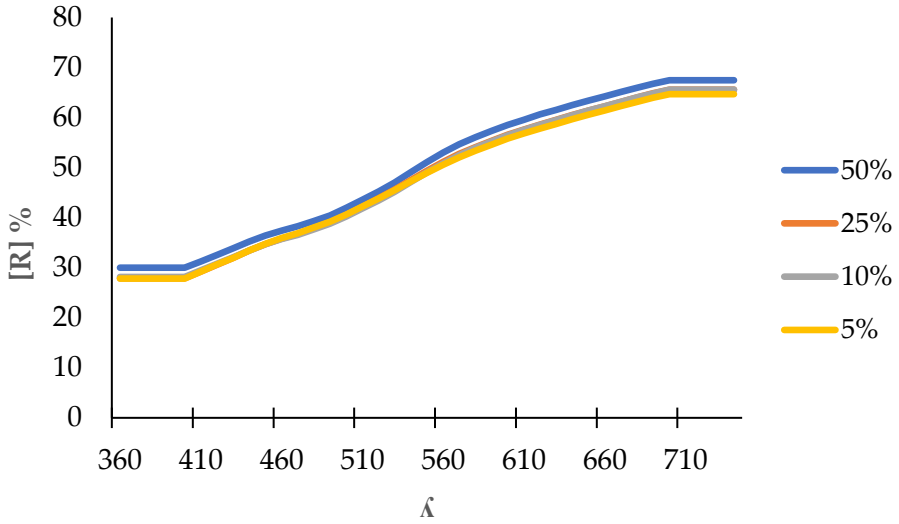

Figure 14. Measurement of reflectance (%) for the cleaning solutions (stone exposed to the sunlight).

In the case of the stone exposed to sunlight, all cleaning solutions produced very similar and effective results, visible both through colorimetric parameters and through reflectance measurement. This is advantageous because it allows for the consideration of using the lowest concentration, which is certainly preferable when treating heritage materials, as it minimizes potential damage while still being effective.

4. Conclusions

Bacterial biofilms frequently cause discoloration on cultural heritage stone monuments, including the pink discoloration on the Batalha Monastery's walls and columns. Using both culture-dependent and -independent methods, we identified key colonizing genera—*Halalkalicoccus*, *Bacillus*, *Gordonia*, *Serratia*, and *Methylobacterium*—as contributors to the biofilms. Techniques like colorimetry and Raman spectroscopy further characterized the pigments and color changes, showing that *Gordonia* biofilms intensified discoloration in sunlight. Cleaning tests on limestone effectively removed the pigments, demonstrating the safety of the solution for heritage use. We believe this study is a crucial step toward developing an accurate and effective conservation and intervention plan (including monitoring and mitigation treatments) for the Batalha Monastery, a UNESCO World Heritage monument.

Author Contributions: Conceptualization, I.S., A.C. and A.T.C.; methodology, C.S., I.S. and A.T.C.; formal analysis, I.S. investigation, I.S, C.S., A.Z.M., A.C. and A.T.C.; writing—original draft preparation, I.S.; writing—review and editing, A.C., A.T.C., C.S. and A.Z.M.; supervision, A.T.C.; funding acquisition, A.T.C., A.C. and C.S. All authors have read and agreed to the published version of the manuscript.

Funding: This work was funded by national funds through the FCT—Foundation for Science and Technology, I.P.—under the projects UI/BD/153582/2022 (I. Silva PhD Grant), C. Salvador (DOI: 10.54499/DL57/2016/CP1372/CT0019), UIDB/04449/2020 (HERCULESLab), IN2PAST (DOI: 10.54499/LA/P/0132/2020), ART3mis (DOI: 10.54499/2022.07303.PTDC), MICROCENO (DOI: 10.54499/PTDC/CTA-AMB/0608/2020), and Old Goa Revelations (DOI: 10.54499/2022.10305.PTDC).

Institutional Review Board Statement: Not applicable.

Informed Consent Statement: Not applicable.

Data Availability Statement: The sequence data presented in this study have been uploaded to the NCBI Sequence Read Archive (SRA) under Bioproject PRJNA1140600 (SRR30203440-SRR30203447 and SRR30203430). These data can be found at https://www.ncbi.nlm.nih.gov/sra/PRJNA1140600 (accessed on 12 August 2024).

Acknowledgments: The authors gratefully acknowledge the City University of Macau endowment to the Sustainable Heritage Chair & Sino-Portugal Joint Laboratory of Cultural Heritage Conservation Science supported by the Belt and Road Initiative. The authors also wish to acknowledge Antónia Tinturé, Direção-Geral do Património Cultural, for allowing them to perform this study.

Conflicts of Interest: The authors declare no conflicts of interest.

References

1. Ding, Y.; Salvador, C.S.C.; Caldeira, A.T.; Angelini, E.; Schiavon, N. Biodegradation and Microbial Contamination of Limestone Surfaces: An Experimental Study from Batalha Monastery, Portugal. *Corros. Mater. Degrad.* **2021**, *2*, 31–45. [CrossRef]
2. Moura Soares, C. The Archival Sources of the Batalha Monastery (Portugal): Unique Collections for the Study of the Monument's Restoration Work in the 19th Century. *An. Hist. Arte* **2022**, *32*, 255–288. [CrossRef]
3. Valadas, S.; Candeias, A.; Dias, C.; Schiavon, N.; Cotovio, M.; Pestana, J.; Gil, M.; Mirão, J. A Multi-Analytical Study of the Fifteenth Century Mural Paintings of the Batalha Monastery (Portugal) in View of Their Conservation. *Appl. Phys. A Mater. Sci. Process.* **2013**, *113*, 989–998. [CrossRef]
4. Ding, Y.; Redol, P.; Angelini, E.; Mirão, J.; Schiavon, N. Surface Orange Patinas on the Limestone of the Batalha Monastery (Portugal): Characterization and Decay Patterns. *Environ. Sci. Pollut. Res.* **2022**, *29*, 29467–29477. [CrossRef]
5. Pyzik, A.; Ciuchcinski, K.; Dziurzynski, M.; Dziewit, L. The Bad and the Good-Microorganisms in Cultural Heritage Environments—An Update on Biodeterioration and Biotreatment Approaches. *Materials* **2021**, *14*, 177. [CrossRef]
6. Gaylarde, C.; Ribas Silva, M.; Warscheid, T. Microbial Impact on Building Materials: An Overview. *Mater. Struct.* **2003**, *36*, 342–352. [CrossRef]
7. Schröder, V.; Carutiu, D.; Honcea, A.; Ion, R.-M. *Microscopical Methods for the In Situ Investigation of Biodegradation on Cultural Heritage*; IntechOpen: London, UK, 2019; pp. 1–18.
8. Sterflinger, K.; Piñar, G. Microbial Deterioration of Cultural Heritage and Works of Art—Tilting at Windmills? *Appl. Microbiol. Biotechnol.* **2013**, *97*, 9637–9646. [CrossRef] [PubMed]
9. Ding, X.; Lan, W.; Gu, J.D. A Review on Sampling Techniques and Analytical Methods for Microbiota of Cultural Properties and Historical Architecture. *Appl. Sci.* **2020**, *10*, 8099. [CrossRef]
10. Cardoni, M.; Caracciolo, A.; Grenni, P. Fluorescence in Situ Hybridization Technique: A Tool Useful for Detecting Cultural Heritage Biodeteriogens. In *Sciences and Technologies Applied to Cultural Heritage*; Baldi, M., Vittozzi, G., Eds.; Elsevier: Amsterdam, The Netherlands, 2019; pp. 34–44.
11. Sandmann, G. Carotenoids and Their Biosynthesis in Fungi. *Molecules* **2022**, *27*, 1431. [CrossRef]
12. Paul, D.; Kumari, P.K.; Siddiqui, N. Yeast Carotenoids: Cost-Effective Fermentation Strategies for Health Care Applications. *Fermentation* **2023**, *9*, 147. [CrossRef]
13. Ljaljević Grbić, M.; Dimkić, I.; Janakiev, T.; Kosel, J.; Tavzes, Č.; Popović, S.; Knežević, A.; Legan, L.; Retko, K.; Ropret, P.; et al. Uncovering the Role of Autochthonous Deteriogenic Biofilm Community: Rožanec Mithraeum Monument (Slovenia). *Microb. Ecol.* **2024**, *87*, 87. [CrossRef] [PubMed]
14. Goga, M.; Elečko, J.; Marcinčinová, M.; Ručová, D.; Bačkorová, M.; Bačkor, M. Lichen Metabolites: An Overview of Some Secondary Metabolites and Their Biological Potential. In *Co-Evolution of Secondary Metabolites*; Merillon, J.-M., Ramawat, K.G., Eds.; Springer: Berlin/Heidelberg, Germany, 2020; pp. 175–209. ISBN 9783319963976.
15. Sajjad, W.; Din, G.; Rafiq, M.; Iqbal, A.; Khan, S.; Zada, S.; Ali, B.; Kang, S. Pigment Production by Cold-Adapted Bacteria and Fungi: Colorful Tale of Cryosphere with Wide Range Applications. *Extremophiles* **2020**, *24*, 447–473. [CrossRef] [PubMed]
16. Silva, T.P.; Paixão, S.M.; Alves, L. Ability of Gordonia Alkanivorans Strain 1B for High Added Value Carotenoids Production. *RSC Adv.* **2016**, *6*, 58055–58063. [CrossRef]
17. Naz, T.; Ullah, S.; Nazir, Y.; Li, S.; Iqbal, B.; Liu, Q.; Mohamed, H.; Song, Y. Industrially Important Fungal Carotenoids: Advancements in Biotechnological Production and Extraction. *J. Fungi* **2023**, *9*, 578. [CrossRef] [PubMed]
18. Cojoc, L.R.; Enache, M.I.; Neagu, S.E.; Lungulescu, M.; Setnescu, R.; Ruginescu, R.; Gomoiu, I. Carotenoids Produced by Halophilic Bacterial Strains on Mural Paintings and Laboratory Conditions. *FEMS Microbiol. Lett.* **2019**, *366*, fnz243. [CrossRef] [PubMed]
19. Rinta-Kanto, J.M.; Ouellette, A.J.A.; Boyer, G.L.; Twiss, M.R.; Bridgeman, T.B.; Wilhelm, S.W. Quantification of Toxic Microcystis Spp. during the 2003 and 2004 Blooms in Western Lake Erie Using Quantitative Real-Time PCR. *Environ. Sci. Technol.* **2005**, *39*, 4198–4205. [CrossRef] [PubMed]
20. Rosado, T.; Dias, L.; Lança, M.; Nogueira, C.; Santos, R.; Martins, M.R.; Candeias, A.; Mirão, J.; Caldeira, A.T. Assessment of Microbiota Present on a Portuguese Historical Stone Convent Using High-Throughput Sequencing Approaches. *Microbiologyopen* **2020**, *9*, 1067–1084. [CrossRef]
21. Salvador, C.; Silva, M.; Rosado, T.; Freire, R.V.; Bordalo, R.; Candeias, A.; Caldeira, A.T. Biodeterioração de Pinturas de Cavalete: Desenvolvimento de Novas Estratégias de Mitigação. *Conserv. Património* **2016**, *23*, 119–124. [CrossRef]
22. Silva, I.; Dias, L.; Salvador, C.; Miller, A.Z.; Candeias, A.; Teresa Caldeira, A. Microbial Induced Stone Discoloration in Alcobaça Monastery: A Comprehensive Study. *J. Cult. Herit.* **2024**, *67*, 248–257. [CrossRef]

23. Rosado, T.; Falé, A.; Gil, M.; Mirão, J.; Candeias, A.; Caldeira, A.T. Understanding the Influence of Microbial Contamination on Colour Alteration of Pigments Used in Wall Paintings—The Case of Red and Yellow Ochres and Ultramarine Blue. *Color Res. Appl.* **2019**, *44*, 783–789. [CrossRef]
24. Goswami, G.; Panda, D.; Samanta, R.; Boro, R.C.; Modi, M.K.; Bujarbaruah, K.M.; Barooah, M. Bacillus Megaterium Adapts to Acid Stress Condition through a Network of Genes: Insight from a Genome-Wide Transcriptome Analysis. *Sci. Rep.* **2018**, *8*, 16105. [CrossRef] [PubMed]
25. Mitchell, C.; Iyer, S.; Skomurski, J.F.; Vary, J.C. Red Pigment in Bacillus Megaterium Spores. *Appl. Environ. Microbiol.* **1986**, *52*, 64–67. [CrossRef] [PubMed]
26. Khaneja, R.; Perez-Fons, L.; Fakhry, S.; Baccigalupi, L.; Steiger, S.; To, E.; Sandmann, G.; Dong, T.C.; Ricca, E.; Fraser, P.D.; et al. Carotenoids Found in Bacillus. *J. Appl. Microbiol.* **2010**, *108*, 1889–1902. [CrossRef] [PubMed]
27. Moeller, R.; Horneck, G.; Facius, R.; Stackebrandt, E. Role of Pigmentation in Protecting *Bacillus* Sp. Endospores against Environmental UV Radiation. *FEMS Microbiol. Ecol.* **2005**, *51*, 231–236. [CrossRef] [PubMed]
28. Kummer, C.; Schumann, P.; Stackebrandt, E. *Gordonia alkanivorans* Sp. Nov., Isolated from Tar-Contaminated Soil. *Int. J. Syst. Bacteriol.* **1999**, *49*, 1513–1522. [CrossRef] [PubMed]
29. Pacheco, M. Production of *Gordonia alkanivorans* Strain 1B Biomass in Bioreactor and Further Application Towards Fossil Fuels Desulfurization. Ph.D. Thesis, Faculdade de Ciências, Universidade De Lisboa, Lisboa, Portugal, 2015.
30. Arenskötter, M.; Bröker, D.; Steinbüchel, A. Biology of the Metabolically Diverse Genus Gordonia. *Appl. Environ. Microbiol.* **2004**, *70*, 3195–3204. [CrossRef]
31. Zhang, C.-X.; Yang, S.-Y.; Xu, M.-X.; Sun, J.; Liu, H.; Liu, J.-R.; Kan, F.; Lai, R.; Zhang, K.-Y. *Serratia nematodiphila* Sp. Nov., Associated Symbiotically with the Entomopathogenic Nematode Heterorhabditidoides Chongmingensis (Rhabditida: Rhabditidae). *Int. J. Syst. Evol. Microbiol.* **2009**, *59*, 1603–1608. [CrossRef]
32. Gondil, V.S.; Asif, M.; Bhalla, T.C. Optimization of Physicochemical Parameters Influencing the Production of Prodigiosin from Serratia Nematodiphila RL2 and Exploring Its Antibacterial Activity. *3 Biotech* **2017**, *7*, 388. [CrossRef] [PubMed]
33. Boers, S.A.; Jansen, R.; Hays, J.P. Understanding and Overcoming the Pitfalls and Biases of Next-Generation Sequencing (NGS) Methods for Use in the Routine Clinical Microbiological Diagnostic Laboratory. *Eur. J. Clin. Microbiol. Infect. Dis.* **2019**, *38*, 1059–1070. [CrossRef]
34. Turnbull, P.C.B. Bacillus. In *Medical Microbiology*; Baron, S., Turnbull, P.C.B., Eds.; University of Texas Medical Branch: Galveston, TX, USA, 1996.
35. Caldeira, T. Green Mitigation Strategy for Cultural Heritage Using Bacterial Biocides. In *Microorganisms in the Deterioration and Preservation of Cultural Heritage*; Joseph, E., Ed.; Springer: Cham, Switzerland, 2021; pp. 137–148. ISBN 978-3-030-69410-4.
36. Capodicasa, S.; Fedi, S.; Porcelli, A.M.; Zannoni, D. The Microbial Community Dwelling on a Biodeteriorated 16th Century Painting. *Int. Biodeterior. Biodegrad.* **2010**, *64*, 727–733. [CrossRef]
37. Kiel, G.; Gaylarde, C.C. Bacterial Diversity in Biofilms on External Surfaces of Historic Buildings in Porto Alegre. *World J. Microbiol. Biotechnol.* **2006**, *22*, 293–297. [CrossRef]
38. Ettenauer, J.D.; Jurado, V.; Piñar, G.; Miller, A.Z.; Santner, M.; Saiz-Jimenez, C.; Sterflinger, K. Halophilic Microorganisms Are Responsible for the Rosy Discolouration of Saline Environments in Three Historical Buildings with Mural Paintings. *PLoS ONE* **2014**, *9*, e103844. [CrossRef] [PubMed]
39. Piñar, G.; Ettenauer, J.; Sterflinger, K. "La Vie En Rose": A Review of the Rosy Discoloration of Subsurface Monuments. In *The Conservation of Subterranean Cultural Heritage*; Saiz-Jimenez, C., Ed.; CRC Press: Boca Raton, FL, USA, 2014; pp. 113–124. ISBN 9781315739977.
40. Tichy, J.; Waldherr, M.; Ortbauer, M.; Graf, A.; Sipek, B.; Jembrih-Simbuerger, D.; Sterflinger, K.; Piñar, G. Pretty in Pink? Complementary Strategies for Analysing Pink Biofilms on Historical Buildings. *Sci. Total Environ.* **2023**, *904*, 166737. [CrossRef] [PubMed]
41. Adamiak, J.; Otlewska, A.; Gutarowska, B. Halophilic Microbial Communities in Deteriorated Buildings. *World J. Microbiol. Biotechnol.* **2015**, *31*, 1489–1499. [CrossRef]
42. Coelho, C.; Mesquita, N.; Costa, I.; Soares, F.; Trovão, J.; Freitas, H.; Portugal, A.; Tiago, I. Bacterial and Archaeal Structural Diversity in Several Biodeterioration Patterns on the Limestone Walls of the Old Cathedral of Coimbra. *Microorganisms* **2021**, *9*, 709. [CrossRef]
43. Wu, F.; Zhang, Y.; He, D.; Gu, J.D.; Guo, Q.; Liu, X.; Duan, Y.; Zhao, J.; Wang, W.; Feng, H. Community Structures of Bacteria and Archaea Associated with the Biodeterioration of Sandstone Sculptures at the Beishiku Temple. *Int. Biodeterior. Biodegrad.* **2021**, *164*, 105290. [CrossRef]
44. Ventosa, A.; Sánchez-Porro, C. *Bergey's Manual of Systematics of Archaea and Bacteria*, 1st ed.; Whitman, W.B., Ed.; John Wiley & Sons, Inc.: Hoboken, NJ, USA, 2017; ISBN 9781118960608.
45. Pane, L.; Radin, L.; Franconi, G.; Carli, A. The Carotenoid Pigments of a Marine Bacillus Firmus Strain. *Boll. Soc. Ital. Biol. Sper.* **1996**, *72*, 303–308. [PubMed]
46. Steiger, S.; Perez-Fons, L.; Fraser, P.D.; Sandmann, G. Biosynthesis of a Novel C 30 Carotenoid in Bacillus Firmus Isolates. *J. Appl. Microbiol.* **2012**, *113*, 888–895. [CrossRef] [PubMed]

47. Ngo, H.T.; Nguyen, T.T.N.; Nguyen, Q.M.; Tran, A.V.; Do, H.T.V.; Nguyen, A.H.; Phan, T.N.; Nguyen, A.T.V. Screening of Pigmented Bacillus Aquimaris SH6 from the Intestinal Tracts of Shrimp to Develop a Novel Feed Supplement for Shrimp. *J. Appl. Microbiol.* **2016**, *121*, 1357–1372. [CrossRef] [PubMed]
48. Shivaji, S.; Chaturvedi, P.; Begum, Z.; Pindi, P.K.; Manorama, R.; Padmanaban, D.A.; Shouche, Y.S.; Pawar, S.; Vaishampayan, P.; Dutt, C.B.S.; et al. Janibacter Hoylei Sp. Nov., Bacillus Isronensis Sp. Nov. and Bacillus Aryabhattai Sp. Nov., Isolated from Cryotubes Used for Collecting Air from the Upper Atmosphere. *Int. J. Syst. Evol. Microbiol.* **2009**, *59*, 2977–2986. [CrossRef]
49. Hong, B.H.; Joe, M.M.; Selvakumar, G.; Kim, K.Y.; Choi, J.H.; Sa, T.M. Influence of Salinity Variations on Exocellular Polysaccharide Production, Biofilm Formation and Flocculation in Halotolerant Bacteria. *J. Environ. Biol.* **2017**, *38*, 657–664. [CrossRef]
50. Pepe, O.; Sannino, L.; Palomba, S.; Anastasio, M.; Blaiotta, G.; Villani, F.; Moschetti, G. Heterotrophic Microorganisms in Deteriorated Medieval Wall Paintings in Southern Italian Churches. *Microbiol. Res.* **2010**, *165*, 21–32. [CrossRef] [PubMed]
51. Jurado, V.; Gonzalez-Pimentel, J.L.; Hermosin, B.; Saiz-Jimenez, C. Biodeterioration of Salón de Reinos, Museo Nacional Del Prado, Madrid, Spain. *Appl. Sci.* **2021**, *11*, 8858. [CrossRef]
52. Skipper, P.J.A.; Skipper, L.K.; Dixon, R.A. A Metagenomic Analysis of the Bacterial Microbiome of Limestone, and the Role of Associated Biofilms in the Biodeterioration of Heritage Stone Surfaces. *Sci. Rep.* **2022**, *12*, 4877. [CrossRef] [PubMed]
53. Ljaljevic-Grbic, M.; Stupar, M.; Savkovic, Z.; Knezevic, A.; Dimkic, I.; Kosel, J.; Tavzes, C.; Unkovic, N. From On-Site to in-Lab: Microscopic Observation of Fungal Proliferation on 17th Century Mural Paintings. *Zb. Matice Srp. Za Prir. Nauk.* **2022**, *143*, 7–14. [CrossRef]
54. Rivera, L.E.C.; Ramos, A.P.; Sánchez, J.I.C.; Drago, M.E. Origin and Control Strategies of Biofilms in the Cultural Heritage. In *Antimicrobials, Antibiotic Resistance, Antibiofilm Strategies and Activity Methods*; Kırmusaoğlu, S., Ed.; IntechOpen: London, UK, 2019; ISBN 978-1-78985-790-0.
55. Ahmed, E.A.-E.; Mohamed, R.M. Bacterial Deterioration in the Limestone Minaret of Prince Muhammad and Suggested Treatment Methods, Akhmim, Egypt. *Geomaterials* **2022**, *12*, 37–58. [CrossRef]
56. Xue, Y.; Fan, H.; Ventosa, A.; Grant, W.D.; Jones, B.E.; Cowan, D.A.; Ma, Y. *Halalkalicoccus tibetensis* Gen. Nov., Sp. Nov., Representing a Novel Genus of Haloalkaliphilic Archaea. *Int. J. Syst. Evol. Microbiol.* **2005**, *55*, 2501–2505. [CrossRef]
57. Amador, C.I.; Stannius, R.O.; Røder, H.L.; Burmølle, M. High-Throughput Screening Alternative to Crystal Violet Biofilm Assay Combining Fluorescence Quantification and Imaging. *J. Microbiol. Methods* **2021**, *190*, 106343. [CrossRef] [PubMed]
58. Wilson, C.; Lukowicz, R.; Merchant, S.; Valquier-Flynn, H.; Caballero, J.; Sandoval, J.; Okuom, M.; Huber, C.; Durham Brooks, T.; Wilson, E.; et al. Quantitative and Qualitative Assessment Methods for Biofilm Growth: A Mini-Review. *Res. Rev. J. Eng. Technol.* **2017**, *6*.
59. Borowicz, M.; Krzyżanowska, D.M.; Jafra, S. Crystal Violet-Based Assay for the Assessment of Bacterial Biofilm Formation in Medical Tubing. *J. Microbiol. Methods* **2023**, *204*, 106656. [CrossRef]
60. Sanmartín, P.; Silva, B.; Prieto, B. Effect of Surface Finish on Roughness, Color, and Gloss of Ornamental Granites. *J. Mater. Civ. Eng.* **2011**, *23*, 1239–1248. [CrossRef]
61. Jeon, B.Y.; Kim, B.Y.; Jung, I.L.; Park, D.H. Metabolic Roles of Carotenoid Produced by Non-Photosynthetic Bacterium Gordonia Alkanivorans SKF120101. *J. Microbiol. Biotechnol.* **2012**, *22*, 1471–1477. [CrossRef] [PubMed]
62. Fernandes, A.S.; Paixão, S.M.; Silva, T.P.; Roseiro, J.C.; Alves, L. Influence of Culture Conditions towards Optimal Carotenoid Production by Gordonia Alkanivorans Strain 1B. *Bioprocess Biosyst. Eng.* **2018**, *41*, 143–155. [CrossRef]
63. Udensi, J.; Loughman, J.; Loskutova, E.; Byrne, H.J. Raman Spectroscopy of Carotenoid Compounds for Clinical Applications—A Review. *Molecules* **2022**, *27*, 9017. [CrossRef] [PubMed]
64. Zha, W.L.; Cheng, Y.; Yu, W.; Zhang, X.B.; Shen, A.G.; Hu, J.M. HPLC Assisted Raman Spectroscopic Studies on Bladder Cancer. *Laser Phys. Lett.* **2015**, *12*, 045701. [CrossRef]
65. Horiue, H.; Sasaki, M.; Yoshikawa, Y.; Toyofuku, M.; Shigeto, S. Raman Spectroscopic Signatures of Carotenoids and Polyenes Enable Label-Free Visualization of Microbial Distributions within Pink Biofilms. *Sci. Rep.* **2020**, *10*, 7704. [CrossRef]
66. Shao, Y.; Gu, W.; Jiang, L.; Zhu, Y. Study on the Visualization of Pigment in Haematococcus Pluvialis by Raman Spectroscopy Technique. *Sci. Rep.* **2019**, *9*, 12097. [CrossRef]
67. Gellermann, W.; Ermakov, I.V.; Ermakova, M.R.; McClane, R.W.; Zhao, D.-Y.; Bernstein, P.S. In Vivo Resonant Raman Measurement of Macular Carotenoid Pigments in the Young and the Aging Human Retina. *J. Opt. Soc. Am. A* **2002**, *19*, 1172. [CrossRef]
68. Arteni, A.A.; Fradot, M.; Galzerano, D.; Mendes-Pinto, M.M.; Sahel, J.A.; Picaud, S.; Robert, B.; Pascal, A.A. Structure and Conformation of the Carotenoids in Human Retinal Macular Pigment. *PLoS ONE* **2015**, *10*, e0135779. [CrossRef] [PubMed]
69. Chen, C.; Huang, W.; Gao, Q.; Fan, L.; Shen Andy, H. Assignments on Raman Peaks of Red Coral Based on Experimental Raman Spectroscopy and Density Functional Theory Calculation. *Spectrosc. Spectr. Anal.* **2021**, *41*, 127. [CrossRef]
70. Ormsby, B.; Bartoletti, A.; van den Berg, K.J.; Stavroudis, C. Cleaning and Conservation: Recent Successes and Challenges. *Herit. Sci.* **2024**, *12*, 10. [CrossRef]
71. Sarti, B.; Villa, F.; Cappitelli, F.; Rizzi, A. Chromatic Bio-Indicators of Biofilm Community Structure on Stone Heritage. In Proceedings of the 15th Congress of the International Colour Association, Chiang Rai, Thailand, 28 November–2 December 2023; pp. 412–418.

72. Wang, Y.; Zhang, H.; Liu, X.; Liu, X.; Song, W. Fungal Communities in the Biofilms Colonizing the Basalt Sculptures of the Leizhou Stone Dogs and Assessment of a Conservation Measure. *Herit. Sci.* **2021**, *9*, 36. [CrossRef]
73. Morgado, D.; Fanesi, A.; Martin, T.; Tebbani, S.; Bernard, O.; Lopes, F. Non-Destructive Monitoring of Microalgae Biofilms. *Bioresour. Technol.* **2024**, *398*, 130520. [CrossRef]